Outdoor weathering and dissolution of TNT and Tritonal

Susan Taylor [a,*], James H. Lever [a], Jennifer Fadden [a], Nancy Perron [a], Bonnie Packer [b]

[a] Cold Regions Research and Engineering Laboratory, 72 Lyme Road, Hanover, NH, United States
[b] US Army Environmental Command, Hoadley Road, Aberdeen Proving Ground, MD 21010, United States

ARTICLE INFO

ABSTRACT

Low-order detonations of military munitions scatter cm-sized chunks of high-explosives onto military range soils, where rainfall can dissolve and then transport the explosives to groundwater. We present 1 year of mass-loss data obtained from cm-sized chunks of the frequently used explosives TNT (2,4,6-trinitrotoluene) and Tritonal (an 80:20 mixture of TNT and aluminum flakes) exposed outdoors to weather and dissolve under natural conditions. The explosive chunks rested on glass frits in individual funnels and all precipitation interacting with them was collected and analyzed. Mass balance data reveal that TNT in the water samples accounts for only about one-third of the TNT lost from the chunks. The creation of photo-transformation products on the solid chunks, and their subsequent dissolution or sublimation, probably accounts for the other two-thirds. Although these products cannot, as yet, be quantified they are intrinsic to the outdoor weathering and fate of TNT-based explosives. TNT in our water samples was not photo-transformed. Thus, we used the yearlong, dissolved-mass time-series to validate a drop-impingement dissolution model for TNT. The model used measured rainfall and air temperature data as input, and the results agreed remarkably well with TNT dissolved-mass time-series measured for the year. This model can estimate annual TNT influx into range soils using annual rainfall and particle-size distributions. Nevertheless, large uncertainties remain in the numbers and sizes of TNT particles scattered on military ranges and the identities and fates of the photo-transformation products.

Published by Elsevier Ltd.

1. Introduction

During live-fire training soldiers fire a variety of munitions under realistic scenarios. Training, however, can produce low-order detonations in addition to intended high-order detonations on military ranges. Low-order detonations scatter many grams of mm-to-cm-sized high-explosive (HE) pieces onto the surface of range soils (Taylor et al., 2004a). These pieces are then available for direct dissolution by rainfall and aqueous transport into groundwater (Clausen et al., 2006; Robertson et al., 2007). Indeed, low-order detonations are thought to be the main source of contamination on ranges today (Taylor et al., 2004b). Because high-explosives such as TNT (2,4,6-trinitrotoluene), and RDX (1,3,5-hexahydro-1,3,5-trinitrotriazine) are toxic (ATSDR, 1995; Mukhi and Patiñoz, 2008) and suspected or known carcinogens, they have low drinking-water screening levels: $2.2\ \mu g\ L^{-1}$ for TNT and $0.6\ \mu g\ L^{-1}$ for RDX (EPA, 2008). Small masses of these explosives can potentially contaminate large volumes of drinking water.

Rainfall-driven dissolution probably controls the time scale over which explosives reach groundwater (Lever et al., 2005; Furey et al., 2008). Aqueous dissolution rates of HE particles have been measured in stirred baths (Lynch et al., 2001, 2002) and in glass-bead columns subjected to porous flow (Phelan et al., 2003). These experiments do not mimic the independent dissolution of HE particles widely separated on the surface of range soils. To mimic these conditions more closely, Lever et al. (2005) conducted laboratory experiments where simulated raindrops fell directly on individual, mm-sized particles of Composition B (Comp B is 60:39:1 mixture of RDX, TNT and wax). They formulated a drop-impingement dissolution model, which predicted the measured dissolved-mass time-series quite well. Extended lab tests showed that this model also works well for small TNT and Tritonal particles (Taylor et al., 2009).

Even at high rainfall rates, gm-to-kg pieces of HE should take many years to dissolve (Lever et al., 2005). However, anecdotal observations suggest that HE chunks are friable and disaggregate into large numbers of smaller particles that dissolve more rapidly, accelerating HE influx into groundwater. Also, solid-phase TNT turns red when exposed outdoors, suggesting that some photo-transformation occurs. To our knowledge, no one has studied how HE particles weather or quantified their dissolution outdoors subject to natural rainfall, sunlight and temperature variations.

We present 1 year of mass-loss data obtained from 11 TNT and five Tritonal cm-sized chunks exposed outdoors. The HE chunks

1. REPORT DATE **OCT 2009**	2. REPORT TYPE	3. DATES COVERED **00-00-2009 to 00-00-2009**
4. TITLE AND SUBTITLE **Outdoor Weathering And Dissolution Of TNT And Tritonal**		5a. CONTRACT NUMBER
		5b. GRANT NUMBER
		5c. PROGRAM ELEMENT NUMBER
6. AUTHOR(S)		5d. PROJECT NUMBER
		5e. TASK NUMBER
		5f. WORK UNIT NUMBER
7. PERFORMING ORGANIZATION NAME(S) AND ADDRESS(ES) **Cold Regions Research and Engineering Laboratory,72 Lyme Road,Hanover,NH,03755**		8. PERFORMING ORGANIZATION REPORT NUMBER
9. SPONSORING/MONITORING AGENCY NAME(S) AND ADDRESS(ES)		10. SPONSOR/MONITOR'S ACRONYM(S)
		11. SPONSOR/MONITOR'S REPORT NUMBER(S)

12. DISTRIBUTION/AVAILABILITY STATEMENT
Approved for public release; distribution unlimited

14. ABSTRACT
Low-order detonations of military munitions scatter cm-sized chunks of high-explosives onto military range soils, where rainfall can dissolve and then transport the explosives to groundwater. We present 1 year of mass-loss data obtained from cm-sized chunks of the frequently used explosives TNT (2,4,6-trinitrotoluene) and Tritonal (an 80:20 mixture of TNT and aluminum flakes) exposed outdoors to weather and dissolve under natural conditions. The explosive chunks rested on glass frits in individual funnels and all precipitation interacting with them was collected and analyzed. Mass balance data reveal that TNT in the water samples accounts for only about one-third of the TNT lost from the chunks. The creation of photo-transformation products on the solid chunks, and their subsequent dissolution or sublimation, probably accounts for the other two-thirds. Although these products cannot, as yet, be quantified they are intrinsic to the outdoor weathering and fate of TNT-based explosives. TNT in our water samples was not photo-transformed. Thus, we used the yearlong, dissolved-mass time-series to validate a drop-impingement dissolution model for TNT. The model used measured rainfall and air temperature data as input, and the results agreed remarkably well with TNT dissolved-mass time-series measured for the year. This model can estimate annual TNT influx into range soils using annual rainfall and particle-size distributions. Nevertheless, large uncertainties remain in the numbers and sizes of TNT particles scattered on military ranges and the identities and fates of the photo-transformation products.

15. SUBJECT TERMS

16. SECURITY CLASSIFICATION OF:			17. LIMITATION OF ABSTRACT	18. NUMBER OF PAGES	19a. NAME OF RESPONSIBLE PERSON
a. REPORT **unclassified**	b. ABSTRACT **unclassified**	c. THIS PAGE **unclassified**	**Same as Report (SAR)**	**8**	

rested on glass frits in individual transparent-glass funnels to remove any soil–TNT interaction and to mimic dissolution of spatially isolated pieces exposed directly to rainfall. Our goals were to measure TNT dissolution by analyzing the rainfall interacting with the HE chunks, to check for mass balance by weighing the chunks periodically, and to document flaking and splitting rates. We also wanted to test the drop-impingement of Lever et al. (2005) to assess its applicability to real-world conditions. We selected TNT because it is a commonly used military explosive, has been found in groundwater under training ranges along with its known breakdown products (Clausen et al., 2006; Bordeleau et al., 2008; Martel et al., 2009) and poses health risks.

2. Materials and methods

Our test site in is a fenced-in outdoor area located in Hanover, New Hampshire, USA. It has a dedicated S-RGA-M00X Hobo tipping-bucket rain gauge and is near an automated weather station, which records rainfall, temperature, wind speed and direction and solar irradiance at 15-min intervals. We calibrated the rain gauge before setting it up outside in April 2006 and used a data logger to record rainfall at 10-min intervals. The gauge was unheated; any recorded snowmelt resulted from above freezing air temperatures.

In May 2006, we placed 11 TNT and five Tritonal chunks outside in 4.0-cm-dia. transparent-glass Buchner funnels, with the chunks resting on glass frits at the bases of the funnels (Fig. 1). The TNT chunks ranged from 0.361 to 1.975 g and the Tritonal chunks ranged from 2.162 to 5.320 g. Each funnel was attached to a 1-L glass bottle with a #4 rubber stopper fitted with two holes, one hole for the funnel stem and the other for a bent copper tube that allows air exchange. The bottles fit snugly into insulated wooden boxes to keep them upright and in the dark, and to moderate temperature variations. Shielding the sample bottles from sunlight is important because aqueous-phase TNT rapidly photo-transforms (Spanggord et al., 1980; Walsh, 1990). To check for photo-transformation in our samples, we placed three solutions of known TNT concentrations in the wooden boxes. These control solutions were analyzed along with our collected samples. Evaporation does not affect dissolved mass collected during the tests, and at no time did the collection bottles overflow with rainwater.

The bottles collected all rainwater or snowmelt that interacted with the HE chunks. About every 10 days, except for the winter months, the bottles were exchanged for clean ones and the water volume and the concentration of explosives were measured. Once the snow covered our experiment, we waited until the spring to exchange the sample bottles. We then archived 20 mL of each sample and collected the remaining water in a waste jug. The sample bottles were then rinsed with a small amount of water, which was also poured into the waste jug, and then rinsed two more times and dried before being re-used. The HE mass in the first rinse contained less than 1% of the mass present in the sample and the two additional rinses ensure that we introduced less than 1% error by reusing the sample bottles.

We weighed the HE chunks approximately monthly using an Ohaus electronic balance and photographed them to document changes in their appearance. This procedure was done after several days of sun and no rain to minimize moisture on the particles. We calibrated the balance before weighing the chunks using 1 g, 10 g and 100 g standards and estimate uncertainties in the measured HE chunks as ±5 mg.

We followed SW-846 Method 8330B (EPA, 2006) to measure the concentrations of TNT and its known breakdown products 1,3,5-trinitrobenzene (1,3,5-TNB), 1,3-dinitrobenzene (DNB), 2,4-dinitrotoluene (2,4-DNT), 2,6-dinitrotoluene (2,6-DNT), 2-amino-4,6-dinitrotoluene (2-ADNT) and 4-amino-2,6-dinitrotoluene (4-ADNT) in the water samples. One milliliter of each water sample was mixed with 2 mL of de-ionized water and 1 mL of acetonitrile and filtered through a 0.45 μm Millipore cartridge. High Performance Liquid Chromatography (HPLC) separated TNT and its co-contaminants using a Water NovaPak C8 column (3.9 mm by 150 mm) eluted at 1.4 mL min^{-1} (28 °C) with 85:15 water:isopropanol mix and detected by UV at 254 nm. Commercially available standards (Restek) specifically developed for Method 8330B were used for calibration. We prepared 1 mg L^{-1} and 10 mg L^{-1} 8095A standards. The 1 mg L^{-1} standard was run every 10 samples and washes were run before and after each standard run. The 10 mg L^{-1} standard was interspersed with the samples as an unknown, and a wash was run after each. The average error for the 10 mg L^{-1}

Fig. 1. Outdoor tests showing Buchner funnels used to hold the HE chunks. Rain landing in the funnel moves through a glass frit and into 1-L glass bottles.

solution run as an unknown was less than 1%. We estimate that cumulative dissolved masses have uncertainties of about ±3% arising mainly from uncertainty in water volume measurements using a graduated cylinder. These methods produced excellent mass balances for laboratory dissolution of HE particles: essentially 100% for TNT and >96% for Comp B (Lever et al., 2005; Taylor et al., 2009).

Hanover, NH, experienced a wet spring and early summer in 2006. Autumn produced few below-freezing temperatures, and no snowfall occurred until January 2007. The experiment was snow covered from mid-January until mid-April, 2007. Total rainfall (including equivalent snowmelt) for the year was 1227 mm. No rain occurred during 95.3% of the time and 54% of the total rainfall fell at rates below 4 mm h^{-1}. The maximum-recorded rainfall rate was 37 mm h^{-1}. The average air temperature was 6.6 °C, and the maximum and minimum temperatures recorded were 33.4 °C and −29.9 °C. Fig. S1 (Supplementary material) shows the air temperature and rainfall rates recorded at the test site during the year.

## 3. Results

3.1. Appearance of HE chunks

Fig. 2 shows, for a TNT and a Tritonal chunk, the initial appearance, the final appearance and a microscopic surface view after 8 months of outdoor exposure. These photo sequences are typical for all 16 chunks tested (Figs. S2 and S3, Supplementary material). The chunks are labeled TNT 1–11 and Tritonal 1–5.

Within 1 month, TNT exposed on the surface of each chunk had turned red due to the effects of sunlight. Interestingly, the TNT chunks became smoother over time whereas the Tritonal chunks became rougher as dissolution exposed the aluminum grains. Cracks appeared in three of the TNT chunks and one of the Tritonal chunks, although none of the chunks split apart. Numerous small particles (about 0.1–1 mm across) flaked off at least seven of the TNT chunks and four of the Tritonal chunks, and their presence increased the surface area of HE available for dissolution. Over the year, the TNT chunks generated more of these small particles than did the Tritonal chunks.

3.2. Mass loss of HE chunks

Table 1 summarizes the mass losses for each HE chunk after 1 year. Total mass loss is from electronic-balance measurements and cumulative dissolved mass is from HPLC analysis for TNT and its known photo-transformation products 1,3,5-TNB, 2-ADNT and 4-ADNT. The latter averaged <3% of the dissolved TNT mass. Figs. S4 and S5 (Supplementary material) show yearlong, dissolved-mass time-series for each chunk.

TNT dissolved mass averaged about one-third of the total TNT mass loss. This result was surprising because we have had excellent HE mass-closure during laboratory dissolution experiments (Lever et al., 2005; Taylor et al., 2009). The unaccounted losses scale closely with surface area (Fig. S6, Supplementary material) and so were smaller for TNT than for Tritonal chunks (37 ± 11 mg versus 62 ± 22 mg). We investigated many pathways for TNT mass
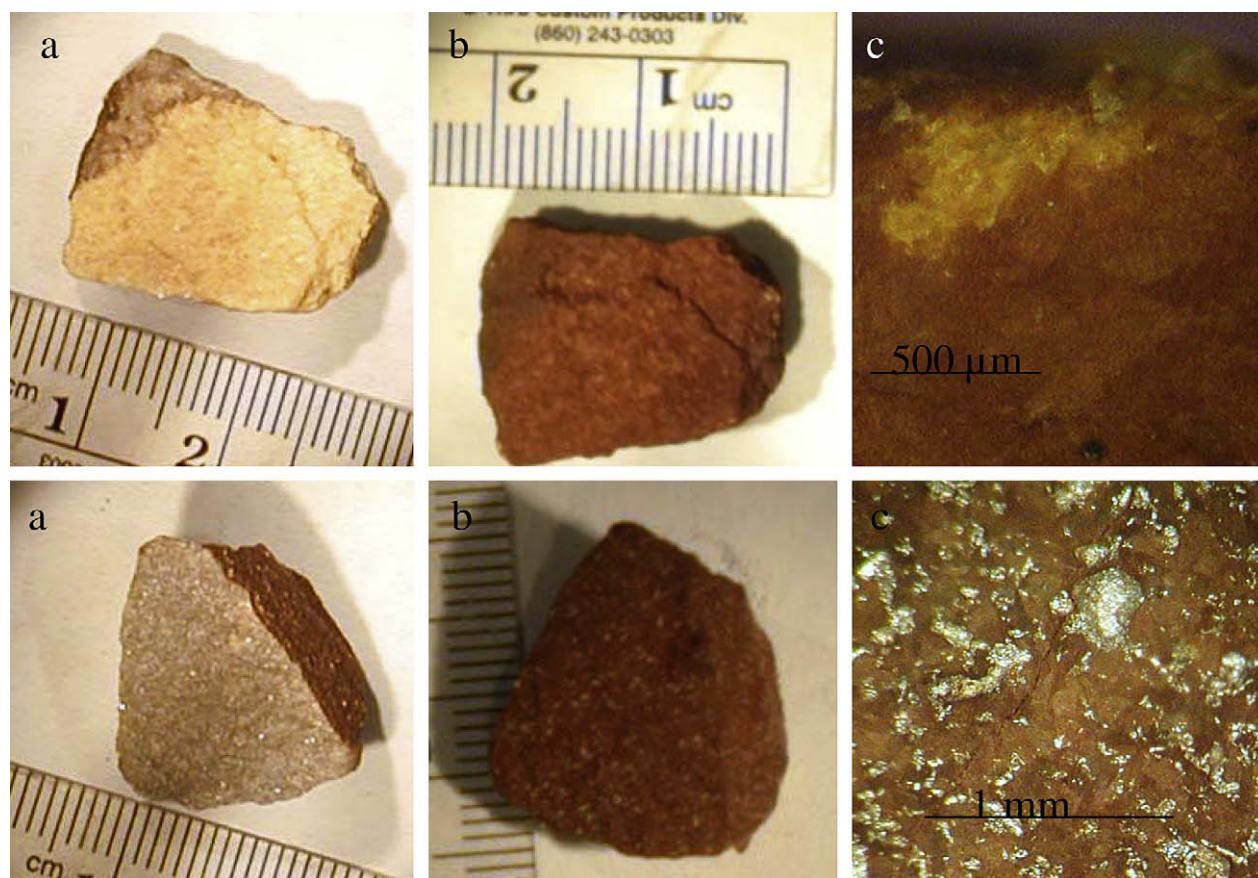
Fig. 2. TNT 4 (upper set) and Tritonal 3 (lower set) photographed in (a) May 2006, (b) May 2007 and (c) December 2006 under a microscope. Microscopic views showed TNT 4 surface was quite smooth but had lost a small flake of the reddish photo-transformed surface, while the Tritonal 3 surface was rougher with exposed aluminum grains and a small crack.

Table 1
Measured mass losses and model area factors for 16 HE chunks exposed outdoors for 1 year. Total TNT mass loss is via electronic balance (corrected for aluminum content of Tritonal), dissolved TNT mass is via HPLC analysis (including measurable transformation products) and unaccounted TNT losses are the difference between these two measurements. Uncertainties are ±0.005 g in total mass loss, ±0.001 g in dissolved TNT mass and ±0.005 g in unaccounted losses. Also shown for each chunk are best-fit area factors and RMS prediction errors for the drop-impingement model (Eq. (7)) and the linear approximation of the drop-impingement model (Eq. (9)).

HE chunk	Electronic balance		HPLC		Drop-impingement model		Linear drop-impingement model	
	Initial mass (g)	Total TNT mass loss (g)	Dissolved TNT mass (g)	Unaccounted TNT mass loss (g)	AF	RMS error	AF1	RMS error
TNT 1	1.975	0.095	0.034	0.061	2.09	0.07	2.17	0.11
TNT 2	0.405	0.045	0.016	0.028	2.43	0.11	2.41	0.14
TNT 3	0.516	0.055	0.023	0.032	2.65	0.06	2.65	0.11
TNT 4	1.371	0.081	0.032	0.049	2.33	0.12	2.38	0.10
TNT 5	0.660	0.050	0.021	0.028	2.26	0.05	2.27	0.13
TNT 6	1.432	0.062	0.021	0.041	1.46	0.09	1.51	0.08
TNT 7	0.946	0.056	0.020	0.035	1.65	0.10	1.69	0.05
TNT 8	0.361	0.036	0.013	0.023	1.77	0.11	1.76	0.10
TNT 9	0.766	0.056	0.020	0.037	1.94	0.08	1.96	0.11
TNT 10	0.647	0.047	0.016	0.031	1.65	0.11	1.67	0.11
TNT 11	1.069	0.064	0.020	0.044	1.51	0.10	1.55	0.06
Average	*0.922*	*0.059*	*0.021*	*0.037*	1.98	0.09	2.00	0.10
St. dev.	*0.501*	*0.017*	*0.006*	*0.011*	0.40		0.38	
Trit 1	2.971	0.073	0.025	0.048	1.24	0.08	1.30	0.09
Trit 2	5.320	0.128	0.028	0.100	0.97	0.06	1.03	0.12
Trit 3	2.466	0.084	0.021	0.063	1.14	0.08	1.18	0.13
Trit 4	2.849	0.079	0.028	0.050	1.46	0.07	1.53	0.14
Trit 5	2.162	0.065	0.018	0.048	1.02	0.10	1.07	0.11
Average	*3.154*	*0.086*	*0.024*	*0.062*	1.17	0.08	1.22	0.12
St. dev.	*1.253*	*0.025*	*0.005*	*0.022*	0.20		0.20	

to leave the particle yet escape HPCL measurement to ensure that such pathways were not defects in the experiment.

Aqueous-phase TNT could have photo-transformed within the sample bottles before their removal from the outdoor boxes (Fig. 1). To assess this, we measured the TNT concentrations in control samples placed in the boxes (two 10 mg L^{-1} and one 1 mg L^{-1} solution). Five-day residence in the box, the average time between rainfall and sample collection, reduced the TNT concentration by less than 0.5%, attesting to the effectiveness of the boxes to exclude sunlight. Additional tests revealed that 5-min exposures to direct sunlight, more than sufficient time to swap the bottles for analysis, reduced TNT concentrations by less than 2%. Also, day-long exposure of the control samples to laboratory lighting produced undetectable changes in the TNT concentrations.

Another pathway for TNT loss is linked to weathering and increased friability of the HE chunks. As noted, weathering produced 0.1–1 mm particles on the frits near many of the chunks. Because we only weighed the main chunks on the electronic balance, the mass of these small particles would be unaccounted for until they dissolved, which would take a couple of months (Lever et al., 2005). However, their individual masses are small (~1 mg for 1-mm particle, 0.001 mg for 0.1-mm particle) and cannot account for the missing TNT mass even if they did not dissolve.

We also assessed whether we inadvertently lost small particles while handling the HE chunks to weigh and photograph them. On seven occasions during the year, each chunk was carefully moved out of the funnel onto weigh-paper on the balance, from there to a glass dish to be photographed, and then back to the funnel, for a total of 21 transfers per HE chunk. To simulate this process, we selected and weighed two HE chunks collected on training ranges but not used for the outdoor tests: 1933.7 ± 0.5 mg TNT and 6147.2 ± 0.5 mg Tritonal. We then transferred them 30 times between two aluminum boats. All four boats contained small particles by the end of the test. The TNT chunk decreased in mass by 1.9 mg and the Tritonal chunk by 7.6 mg. Scaling the mass losses by chunk mass, these handling losses would account for less than 5% of the unaccounted TNT mass losses. This is a conservative estimate because we returned to the funnels any particles that

we observed to flake off the chunks during weighing and photographing.

These control tests indicate that sample collection and particle handling cannot account for the missing TNT mass. That is, the collected water samples represent, within about ±3%, the TNT dissolved from the chunks. About two-thirds of the measured mass loss must have occurred through other processes intrinsic to outdoor exposure of TNT.

Formation and dissolution of reddish photo-transformation products is an intrinsic mass-loss pathway for TNT-based explosives exposed outdoors. As noted, the HE chunks quickly turned reddish after being placed outdoors (Fig. 2), and aqueous-phase TNT is known to photo-transform quickly to form reddish products in solution (Spanggord et al., 1980). Interestingly, the effluent from our outdoor tests always appeared reddish, with visual intensities that correlated with TNT concentrations, and rainfall frequently reduced the reddish appearance of the chunks. Because aqueous-phase TNT transformation was small within our sample bottles, rainfall apparently dissolved, at least partially, the surface red layers into the captured effluent.

Unfortunately, these "red products" have not been unambiguously identified, and Method 8330B does not quantify their aqueous concentrations. To account for the missing TNT mass, red-product layers only 2–3 μm thick would need to form and be dissolved by rainfall between sample collections. To determine whether this is likely, we placed fresh TNT particles in a lab window for several days and then sectioned them. The brick-red photo-transformation product was clearly visible on the exteriors of the particles. Sectioning revealed the red layer to be ~2 μm thick although they are highly variable (Fig. S7, Supplementary material). Furthermore, the red products appear more soluble in water than TNT. We think that solid-phase TNT photo-transforms into soluble compounds that are dissolved by rainfall and that this process probably accounts for the majority of the missing TNT mass.

Sublimation of solid-phase TNT is also a mass-loss pathway intrinsic to outdoor exposure of the HE chunks. However, the vapor pressure of TNT is low, about 1.6×10^{-4} Pa at 20 °C (Legget et al.,

1977; Dionne et al., 1986) and drops exponentially with decreasing temperature. Also, the HE chunks rested at the bottom of 4-cm-dia. × 6-cm-deep funnels and thus were sheltered from the wind. We may estimate the sublimated mass by assuming 1-D diffusion of TNT, from equilibrium concentration at the base of the funnel to zero at the top (Skelland, 1974; Parmeter et al., 1996). This predicts ∼0.1 mg of TNT lost through sublimation for each TNT or Tritonal chunk over the year. Using vapor pressure at 20 °C makes this estimate conservative, but air exchange within the funnels would increase mass loss. Nevertheless, sublimation would need to be two orders-of-magnitude higher for it to be a significant pathway for TNT mass loss from the chunks. Sublimation of aqueous-phase TNT from the sample bottles would be even smaller owing to the small diameter of the vent tubes. Note that these results pertain to our experiment. Sublimation might be important for HE chunks exposed directly to wind on range soils or for photo-transformation products with much higher vapor pressures than TNT.

3.3. Modeling outdoor dissolution

Because TNT concentration in our samples was minimally affected by photo-transformation, the dissolved-mass time-series represent yearlong datasets to validate HE dissolution models. Lever et al. (2005) developed a "drop-impingement" model to predict the dissolution of mm-sized Comp B particles. It pertains to the practical case where spatially isolated HE particles reside on well-draining surface soils and thus are exposed to direct impingement by raindrops. This model assumes that a particle holds a thin (∼0.1 mm) water film against its surface, which saturates with HE between impinging raindrops. For particles smaller than a few milligrams, the volume of typical raindrops exceeds the volume of this water film, and each raindrop refreshes the entire film when it impinges on the particle. In this case, the dissolution rate, m_j (g s^{-1}), is

$$m_j = \frac{S_j V_f}{t_d} \quad (1)$$

where S_j is the solubility limit of species j in water (g cm^{-3}), V_f is the water film volume (cm^3) and t_d is the drop-arrival time (s). Lever et al. (2005) formulated the model with V_f evaluated for a film of thickness h against a spherical particle of equivalent mass as the particle of interest:

$$V_f = \frac{4}{3}\pi[(a+h)^3 - a^3] \quad (2)$$

where a is particle radius. They found that the $h \sim 0.1$–0.2 mm produced good agreement with the measured dissolution time-series for four Comp B particles. Recent laboratory tests showed that the model gave excellent agreement with dissolution data for milligram TNT and Tritonal particles, with h averaging 0.086 ± 0.009 mm (Taylor et al., 2009).

We must extend this model to apply it to the larger HE chunks and natural rainfall of the outdoor tests. For particles larger than a few milligrams, the volume of the water film against the particle exceeds typical raindrop volumes. Thus, impinging raindrops contribute to the film but do not completely refresh it. We may assume that, in steady-state conditions, each impinging drop causes an equal volume of HE-saturated water to drip off the particle. In this case, the dissolution rate is

$$m_j = \frac{S_j V_d}{t_d} \quad (3)$$

where V_d is the raindrop volume (cm^3).

The drop-arrival time for either small- or large-particle regime is related to the volumetric flow rate of rainfall impinging on the particle, $A_c q$:

$$t_d = \frac{V_d}{A_c q} \quad (4)$$

where A_c is the rainfall-capture area of the particle (cm^2) and q is rainfall rate (cm s^{-1}). We again model the particle as a sphere of equivalent mass, and we assume that drops able to touch the sphere contribute to the water film. Thus, the rainfall-capture area is a circle with radius equal to the sphere radius plus one drop diameter:

$$A_c = \pi(a + D_{0m})^2 \quad (5)$$

where D_{0m} is the mass-weighted mean diameter for the raindrops. Pruppacher and Klett (1997) indicate that no single spectrum fits all measurements of raindrop sizes, but an exponential drop-size spectrum has frequently been used and provides reasonable fit. In this case

$$D_{0m} = 0.98 R^{0.21} \quad (6)$$

where D_{0m} is in mm for rainfall rate R in mm h^{-1}. Drops sizes thus show a weak dependence on rainfall rate, with $D_{0m} \sim 1$–2 mm for $R \sim 1$–30 mm h^{-1}.

We may then combine Eqs. (3)–(5) to obtain the dissolution rate for the drop-impingement model in the large-particle regime:

$$m_j = S_j \pi(a + D_{0m})^2 q \times AF \quad (7)$$

Following Lever et al. (2005), we include an area factor, AF, in equation (7). In principle, $AF \sim 2$ should account for blocky particle shapes with capture areas larger than an equivalent sphere. In reality, AF is a parameter obtained by best-fit to dissolution data for actual HE chunks.

The transition between the small- and large-particle regimes of the model occurs when V_f exceeds V_d, where V_f is given by Eq. (2) and $V_d = \pi/6 D_{0m}^3$. The median rainfall rate during the first year of outdoor tests was about 4 mm h^{-1}, corresponding to $D_{0m} \sim 1.3$ mm. Lab tests (Lever et al., 2005; Taylor et al., 2009) suggest $h \sim 0.1$ mm for small HE particles. For these conditions, the large-particle regime would apply for TNT and Tritonal particles larger than about 5 mg. All HE chunks studied here far exceeded this size.

Eq. (7) has an important physical interpretation: all the rainfall intercepted by the particle flows off it fully saturated with HE. This can only be true if the average time raindrops reside within water film, $t_r = V_f/A_c q$, is longer than the time required to saturate the film with HE via diffusion, t_s. Lever et al. (2005) argued that the water layer will saturate for $t_s > h^2/D_j$. For $D_{TNT} \sim 4.6 \times 10^6$ cm^2 s^{-1} at 10.5 °C (the 1-year average air temperature weighted by rainfall) and $h \sim 0.1$ mm, saturation time is $t_s \sim 20$ s independent of particle size. At the large-particle boundary of 5 mg, raindrop residence time is $t_r \sim 70$ s for both TNT and Tritonal, and it exceeds 200 s for the smallest chunk studied here (0.36 g). That is, there was sufficient time for raindrops impinging on the chunks to saturate with TNT before dripping off, as required.

3.4. Validation of dissolution model

We ran the drop-impingement model for all TNT and Tritonal chunks using their initial masses, a density value of 1.65 g cm^{-3} for TNT (AMC, 1971) and measured precipitation and temperature data. The starting time was 11 am on 2 May 2006, the end time was 1 year later, and the time step was 10 min (the collection interval for weather data). Over this period, we collected and analyzed 26 sets of effluent samples for each of the 16 HE chunks and used these results to validate the model.

The predicted dissolution rate (Eq. (7)) requires the solubility limit of TNT, S_{TNT}, which varies with temperature. We assumed that the raindrops and the water film on the particle are at the

measured air temperature and used the temperature correlation developed by Lynch et al. (2002):

$$S_{TNT} = \exp\left(16.981 - \frac{3607.5\ \mathrm{K}}{T}\right) \tag{8}$$

where S_{TNT} has units mg L^{-1} and T is air temperature in K. Note that for $T < 0\ °C$, we set S_{TNT} to 0.

Fig. 3 compares predicted and measured TNT dissolved mass for TNT chunks 1 and 11 and Tritonal chunks 1 and 5 over the year. The model shows very good agreement with the data using independent values of area factor (AF) best-fit to the year's measurements. The flat sections on both plots (days 251–307) represent zero dissolution during winter, as expected. Fig. 3 is typical of the agreement achieved by the model with the measurements for all 16 HE chunks (Figs. S8–S15, Supplementary material). Table 1 summarizes the best-fit values of AF determined for each chunk and the resulting prediction errors. Root mean square (RMS) errors average only 8–9% of measured dissolved mass losses.

The area factor does not appear to vary systematically with particle mass for either TNT or Tritonal chunks. However, the AF values are substantially higher for TNT compared with Tritonal. These factors include the effect of minor flaking of HE crystals from the main chunks onto the glass frits, which increased exposed surface area. The more common flaking observed for TNT chunks probably accounts for their larger area factors.

The drop-impingement model has a linear relationship between dissolution rate and rainfall rate (Eq. (7)) ignoring the small effect of rainfall rate on drop diameter. That is, cumulative mass loss is approximately proportional to cumulative rainfall independent of rate:

$$M_{lossj}(t) = \int_0^t m_j dt = \pi AF \int_0^t S_j(a + D_{0m})^2 q\, dt$$
$$\approx \pi AF \overline{S_j}(a_0 + \overline{D_{0m}})^2 H(t) \tag{9}$$

where $H(t)$ is cumulative rainfall (cm) and $\overline{S_j}$ and $\overline{D_{0m}}$ are the average values, weighted by rainfall, of solubility and drop size, respectively. Because particle mass and thus radius change little over a year, Eq. (9) uses the initial radius, a_0.

We implemented this approximate model because it offers a simple approach to estimate HE influx into range soils based on local climatology (rather than rain and temperature time-series). The rainfall-weighted average temperature during the year was 10.5 °C, so $\overline{S_{TNT}} = 7.1 \times 10^{-5}$ g cm^{-3} via Eq. (8). About 54% of total rainfall fell at rates below 4 mm h^{-1} and 90% fell at rates below 13 mm h^{-1}. These rates produce mean drop sizes of 0.13–0.17 cm via Eq. (6). Estimated mass loss (Eq. (9)) is not very sensitive to mean drop size. We selected $\overline{D_{0m}} = 0.17$ cm because large drops contribute slightly more to mass loss, and the best-fit area factors match those obtained from the complete drop-impingement model. Table 1 includes the resulting area factors, termed AF1, and the RMS prediction errors for the approximate model, which average only slightly larger than those for the complete drop-impingement model. Fig. 4 shows the linear approximation compared with measured data for TNT 1 and Tritonal 1 over the year. The linear approximation does not follow the seasonal variations in dissolution because it uses a constant solubility. Nevertheless, its simplicity is a distinct advantage.

The approximate drop-impingement model also allows us to estimate lifespan of HE particles on ranges by allowing particle radius to vary but retaining average solubility and drop size. Eq. (7) thus becomes

$$m_j = -\frac{dM_j}{dt} = -4\pi \rho_j a^2 \frac{da}{dt} \approx \pi AF \overline{S_j}(a + \overline{D_{0m}})^2 q \tag{10}$$

Rearranging Eq. (10) yields

$$\int_{a(t)}^{a_0} \frac{a^2 da}{(a + \overline{D_{0m}})^2} \approx \frac{AF\overline{S_j}}{4\rho_j} H(t) \tag{11}$$

The rainfall needed to dissolve the particle completely, H_0, is thus
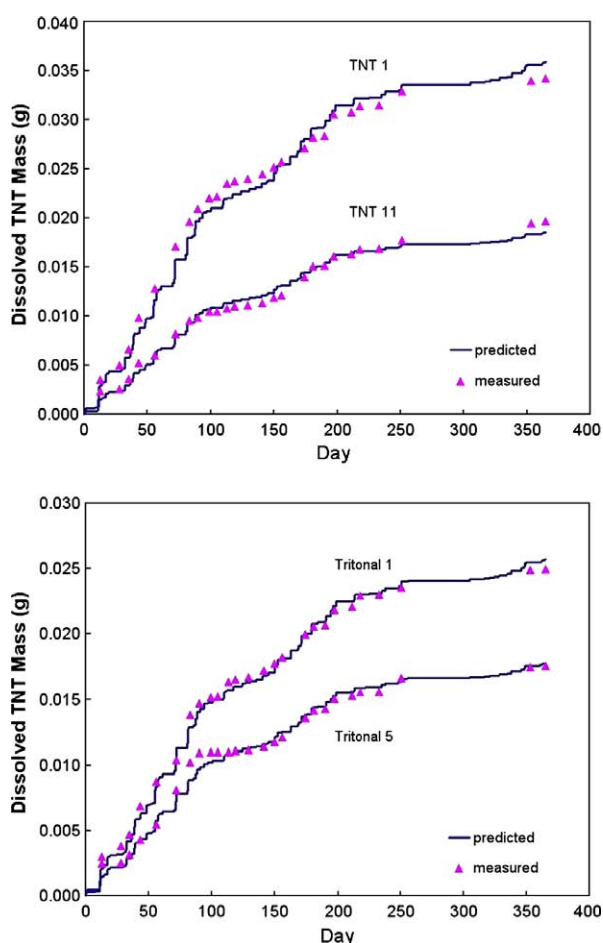

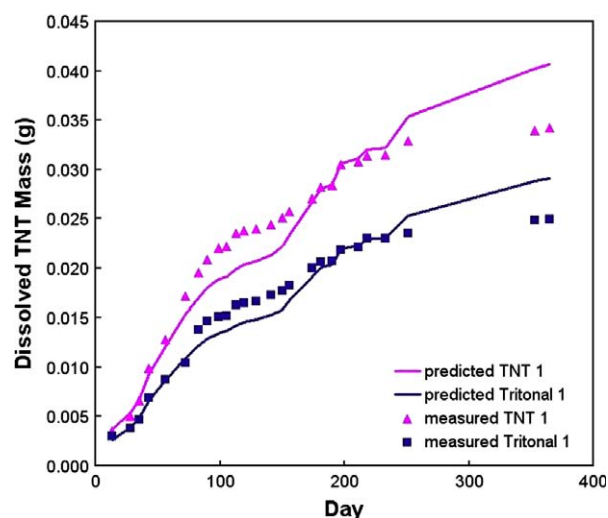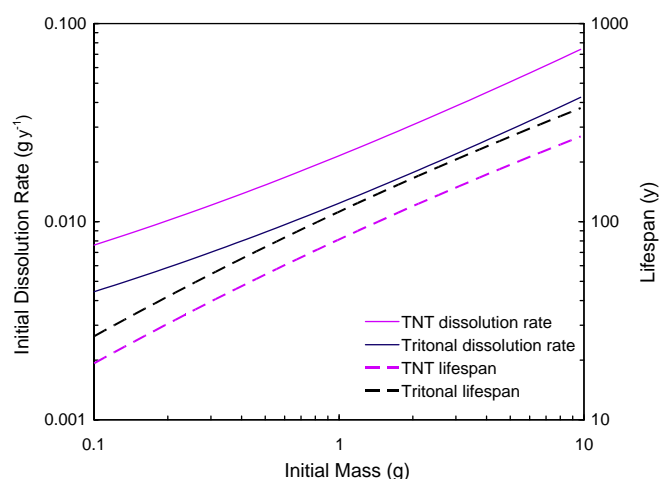Fig. 3. Predicted and measured dissolved TNT mass for four HE chunks.

Fig. 4. Linear approximation of drop-impingement model (Eq. (9)) applied to predict dissolved mass of TNT 1 and Tritonal 1 versus time.

Fig. 5. Initial dissolution rate and particle lifespan versus initial mass, estimated using the approximate drop-impingement model (Eqs. (10) and (12)) for annual average temperature of 10.5 °C and annual rainfall of 100 cm year⁻¹. These estimates do not include mass loss by processes other than TNT dissolution (e.g., photo-transformation, sublimation).

$$H_0 \approx \frac{4\rho_j}{AFS_j} \left\{ \overline{D_{0m}} + a_0 - 2\overline{D_{0m}} \ln\left(1 + \frac{a_0}{\overline{D_{0m}}}\right) - \frac{\overline{D_{0m}}^2}{\overline{D_{0m}} + a_0} \right\} \qquad (12)$$

We may divide H_0 by annual average rainfall, $\overline{H}$, to estimate the lifespan of the particle, t_0 in years. Fig. 5 shows initial dissolution rate and lifespan versus initial particle mass for annual average temperature of 10.5 °C and annual rainfall of 100 cm year⁻¹. The results scale linearly with rainfall rates and solubility. Roughly speaking, 1 g chunks of TNT or Tritonal will require ~100 years to dissolve at annual rainfall of 100 cm year⁻¹ and 200 years at 50 cm year⁻¹. Mass loss by processes other than TNT dissolution (e.g., photo-transformation, sublimation) if they occur at rates similar to those measured here, would reduce these lifespan estimates by about a factor of three.

4. Discussion

These outdoor experiments are the first to mimic the natural weathering and dissolution of TNT and Tritonal chunks scattered onto soils of military training ranges. By placing the HE chunks on glass frits within individual funnels, we were able to observe weathering effects and quantify dissolution without the complicating effects of HE–soil interactions. The sample bottles captured all precipitation that interacted with the HE present in the funnels, namely the main chunks and any pieces that flaked off as a result of weathering.

Because we sought to document changes in the appearance of HE chunks and to check for mass balance, we periodically photographed and weighed them. This revealed an important finding: dissolved TNT mass represented only about one-third of the mass losses from the chunks. We think that formation and dissolution of TNT photo-transformation products, or "red products" on the surface of the chunks, can account for most of the missing two-thirds mass losses. Whether these products occur solely due to radiation or are mediated by moisture on the particle surface is not yet known. Also, sublimation of these products could be important if they are substantially more volatile than TNT. Further study is needed to identify the "red products", develop methods to quantify their concentrations, assess their environmental and health impacts, and measure and model their rates of production and dissolution. Depending on local climate conditions, this pathway could produce the dominant aqueous-phase HE influx into soils. For conditions similar to those of our study site, aqueous-phase red-product influx into range soils could be twice as large as the influx of TNT itself. The drop-impingement model would be able to estimate the dissolution rates of these transformation products once their production rates and solubilities were known.

Because the TNT concentrations in the water samples were minimally affected by photo-transformation, the HPLC measurements accurately reflect the TNT dissolved from each chunk over the yearlong tests. They thus represent an important dataset to validate dissolution models for HE chunks on training ranges. The drop-impingement model predicts the TNT dissolved-mass time-series with remarkably low RMS prediction errors (8–9%) for both TNT and Tritonal chunks using area factor as the only fitting parameter. The model has a simple physical interpretation: all rainfall captured by the particle flows off it fully saturated in HE. The nearly linear relationship between dissolution rate and rainfall rate makes it possible to link average annual HE influx to average annual rainfall. This approximation predicts dissolved mass with only 10–12% RMS errors and can be applied easily to ranges across the country using readily available rainfall and temperature climatology. Slightly larger uncertainties exist in area factors for individual HE particles (±20%) reflecting unknown differences in particle shapes and surface friability. Because large cracks have appeared in several of the HE chunks, it is likely that some or all will split during their lifespans. Splitting into multiple, cm- and mm-sized particles would produce a step increase in exposed surface area not accounted for by average area factors. Continuation of these tests should yield data on the rate of splitting, its dependence on weather conditions, and the size distribution of the resulting group of "daughter" particles.

Probably the largest source of uncertainty to estimating HE aqueous influx into range soils results from the poorly quantified population distribution of the HE particles on a range of interest. The number and size distribution of these particles depends on many factors including the munitions used, how many were fired, their detonation probabilities (high-order, low-order or dud) and weathering and mechanical dissaggregation (Taylor et al., 2004a). It is likely that poor constraint of the number and size distribution of HE particles on a given range could cause an order-of-magnitude uncertainty in predicted annual HE dissolution.

Appendix A. Supplementary material

Supplementary data associated with this article can be found, in the online version, at doi:10.1016/j.chemosphere.2009.09.040.

References

Army Materiel Command, 1971. Engineering Design Handbook: Explosives Series Properties of Explosives of Military Interest. Army Materiel Command, Alexandria, VA.
ATSDR, 1995. Toxicological Profile for 2,4,6-Trinitrotoluene and RDX. US Department of Health and Human Services, Public Health Service, Agency for Toxic Substances and Disease Registry, Atlanta, GA.
Bordeleau, G., Martel, R., Ampleman, G., Thiboutot, S., Jenkins, T.F., 2008. Environmental impacts of training activities at an air weapons range. J. Environ. Qual. 37, 308–317.

Clausen, J.L., Korte, N., Dodson, M., Robb, J., Rieven, S., 2006. Conceptual Model for the Transport of Energetic Residues from Surface Soil to Groundwater by Range Activities. ERDC-CRREL TM-06-18.

Dionne, B.C., Rounbehler, D.P., Achter, E.K., Hobbs, J.R., Fine, D.H., 1986. Vapor pressure of explosives. J. Energ. Mater. 4, 447–472.

Environmental Protection Agency – EPA, 2006. Nitroaromatics, Nitramines and Nitrate Esters by HPLC, SW-846 Method 8330B.

Environmental Protection Agency – EPA, 2008. Region 6 Human Health Medium-Specific Screening Levels. <http://www.epa.gov/Region6/6pd/rcra_c/pd-n/screen.htm>.

Furey, J.S., Fredrickson, H.L., Richmond, M.J., Michel, M., 2008. Effective elution of RDX and TNT from particles of Comp B in surface soil. Chemosphere 70, 1175–1181.

Leggett, D.C, Jenkins, T.F., Murrmann, R.P., 1977. Composition of Vapors Evolved from Military TNT as Influenced by Temperature, Solid Composition, Age and Source. Special Report 77-16, Cold Regions Research and Engineering Laboratory, Hanover, NH.

Lever, J., Taylor, S., Perovich, L., Bjella, K., Packer, B., 2005. Dissolution of Composition B residuals. Environ. Sci. Technol. 39, 8803–8811.

Lynch, J.C., Myers, K., Brannon, J.M., Delfino, J.J., 2001. Effects of pH and temperature on the aqueous solubility and dissolution rate of 2,4,6-trinitrotoluene (TNT), hexahydro-1,3,5-trinitro-1,3,5-triazine (RDX) and octahydro-1,3,5,7-tetranitro-1,3,5,7-tetraazicine (HMX). J. Chem. Eng. Data 46, 1549–1555.

Lynch, J.C., Brannon, J.M., Delfino, J.J., 2002. Dissolution rates of three high explosive compounds: TNT, RDX and HMX. Chemosphere 47, 725–734.

Martel, R., Mailloux, M., Gabriel, U., Lefebvre, R., Ampleman, G., Thiboutot, S., 2009. Behavior of energetic materials in groundwater at an anti-tank range. J. Environ. Qual. 38, 75–92.

Mukhi, S., Patiñoz, R., 2008. Effects of hexahydro-1,3,5-trinitro-1,3,5-triazine (RDX) in zebrafish: general and reproductive toxicity. Chemosphere 72, 726–732.

Parmeter, J.E., Eiceman, G.A., Preston, D.A., Tiano, G.S., 1996. Calibration of an Explosives Vapor Generator Based on Vapor Diffusion from a Condensed Phase. Sandia National Laboratory Technical Report SAN096-2016C.

Phelan, J.M., Webb, S.W., Romero, J.V., Barnett, J.L., Griffin, F., Eliassi, M., 2003. Measurement and Modeling of Energetic Material Mass Transfer to Soil Pore Water – Project CP-1227, Sandia Report 2003-0153.

Pruppacher, H.R., Klett, J.D., 1997. Microphysics of Clouds and Precipitation. Kluwer Academic Publishers, Boston.

Robertson, T.J., Martel, R., Quan, D.M., Ampleman, G., Thiboutot, S., Jenkins, T., Provatas, A., 2007. Fate and transport of 2,4,6-trinitrotoluene in loams at a former explosives factory. Soil Sediment Contam. 16, 159–179.

Skelland, A.H.P., 1974. Diffusional Mass Transfer. Wiley & Sons, New York.

Spanggord, R.J., Mill, T., Chou, T.-W., Mabey, W.R., Smith, J.H., Lee, S., 1980. Environmental Fate Studies on Certain Munition Wastewater Constituents – Phase 1 and 11. Contract Report to US Army Medical Research and Development Center.

Taylor, S., Hewitt, A., Lever, J.H., Hayes, C., Perovich, L., Thorne, P., Daghlian, C., 2004a. TNT particle size distributions from detonated 155-mm howitzer rounds. Chemosphere 55, 357–367.

Taylor, S., Lever, J.H, Bostick, B., Walsh, M.R., Walsh, M.E., Packer, B., 2004b. Underground UXO: Do They Represent a Significant Source of Explosives in Soil Compared to Military Training on Ranges? ERDC/CRREL Technical Report TR-04-23.

Taylor, S., Lever, J.H., Fadden, J., Perron, N., Packer, B., 2009. Simulated rainfall-driven dissolution of TNT, Tritonal, Comp B and Octol particles. Chemosphere 75, 1074–1081.

Walsh, M.E., 1990. Environmental Transformation Products of Nitroaromatics and Nitramines. Special Report 90-2. USACRREL.